19th Brazilian Congress of Thermal Sciences and Engineering
November 6th–10th, 2022, Bento Gonçalves - RS - Brazil

ENC-2022-0247
VALIDATION OF IMERSPEC2D USING GREEN-TAYLOR VORTICES AND TEMPORAL JET

Thiago Fernando Santiago de Freitas
Aristeu da Silveira Neto
Faculdade de Engenharia Mecânica, Universidade Federal de Uberlândia,João Naves de Ávila Avenue, 2121, Sta Mônica, 38400-902, Uberlândia, MG, Brazil
thiago.santiago@ufu.br and aristeus@ufu.br

Felipe Pamplona Mariano
Escola de Engenharia: Elétrica, Mecânica e de Computação, Universidade Federal de Goiás, Ingá Avenue, B5 Building, Samambaia Campus, 74690-900, Goiânia, Goiás, Brazil
fpmariano@ufg.br

Abstract. *The present paper shows the simulations of Taylor-Green vortices and temporal jet using the IMERSPEC2D algorithm. The Taylor-Green vortices are simulated to compare the computational solution obtained by the IMERSPEC2D to a manufactured solution, in order to verify the computational code. Jets are frequently found in nature or in industrial applications such as component mixing processes, thermal transfer, lubrication and deicing, fuel injection in combustion chambers and aircraft propulsion systems, therefore the computational simulations can help in the comprehension and/or evolution of the flow formulation. The IMERSPEC2D solves the continuity equation and linear momentum equations numerically implementing the Pseudo-Spectral Fourier Method (PFM) with the use of the Discrete Fourier Transform (DFT) and the Immersed Boundary Method (IBM). This approach permits performing computational simulations in regular orthogonal uniform meshes and achieving machine error with relatively low computational cost when compared to other spectral methodologies. The reduced computational cost is achieved by the use of DFT as well as the pseudo-spectral approach which does not solve the convolution product of the advective term found in momentum linear equations. Furthermore, the mathematical process of pressure projection replaces the solution of Poisson Equation to vector-matrix multiplication, ensuring the mass balance. The Taylor-Green vortices simulations results show the machine error (errors with 10E(-15) magnitude) with and without the use of IBM while the temporal jet simulations results show good agreement of the 2D simulations and the 3D until the three-dimensionalization of the flow. The formation of eddies is presented for flows with different levels of perturbation in the inlet boundary conditions. The use of different levels of perturbations in the initial condition flow to model temporal jet in transition to turbulence was discovered as a necessity since the high accuracy of the spectral approach. Without inserting small perturbations, the flow does not transition to turbulence neither generate the expected turbulent structures in the flow.*

Keywords: *Green-Taylor Vortices, Jet Flow, Immersed Boundary Method, Pseudo-Spectral Method*

1. INTRODUCTION

In the present paper the IMERSPEC2D code pass over a verification and validation. The code uses the IMERSPEC approach which was proposed by Mariano (2011) for two-dimensional and Moreira (2007) for three-dimensional flows modeling.

Common spectral methodologies applied in Computational Fluid Dynamics (CFD) offers high accuracy at significant computational cost. The IMERSPEC methodology uses a Fourier pseudo-spectral approach whose is able to unify high accuracy and relative low computational cost. Other characteristic of this method is the decoupling pressure of the computational-numerical solution since part of the resolution is made in the spectral domain where it has its own properties.

The present paper is organized as follows: first the mathematical modeling and computational-numerical approach used is presented, next the results are analyzed and compared with other authors and, ultimately conclusions are made.

2. METHODOLOGY

In this section it is appointed the mathematical and numeric-computational methodology approach used. The method used into the simulations is the IMERSPEC which may use two simultaneous domains: an eulerian (Ω) and a lagrangian (Γ) one. The fluid is modeled into the eulerian domain with the Pseudo-Spectral Fourier Method (PFM) and the lagrangian domain is used to complement conditions or characteristics into the flow using the Immersed Boundary Method (IBM).

2.1 Mathematical Methodology

In the present paper, the continuity equation was used to model the flow behavior, Eq. 1,

$$\frac{\partial u_j}{\partial x_j} = 0, \tag{1}$$

and the two-dimensional form of linear momentum equations, Eq. 2,

$$\frac{\partial u_i}{\partial t} + \frac{1}{2}\left[\frac{\partial (u_i u_j)}{\partial x_j} + u_j \frac{\partial u_i}{\partial x_j}\right] = -\frac{\partial p}{\partial x_i} + \nu \frac{\partial^2 u_i}{\partial x_i \partial x_j} + f_i, \tag{2}$$

where $p = p^*/\rho_f$ which p^* is the static pressure in *Pa* and ρ_f is the density in kg/m^3, u_i is the velocity in the i direction in m/s, f_i is a source term f^* in N/m^3 divided by the density ρ_f, ν is the kinematics viscosity in m^2/s, x_i is the spatial component in m and t is the time in s.

The source term is defined in all domain Ω according to the Eq. 3,

$$f_i(\vec{x}, t) = \begin{cases} F_i(\vec{x}, t) & \text{if } \vec{x} = \vec{X_k} \\ 0 & \text{if } \vec{x} \neq \vec{X_k} \end{cases}. \tag{3}$$

The source term represents the influence of the immersed geometry into the flow, thus $f_i(\vec{x}, t)$ is different than zero only in the interface between the immersed body and the fluid flow.

2.2 Pseudo-Spectral Fourier Method

The Equations 1 and 2 are not solved only in the physical space. The IMERSPEC uses the physical and spectral space to solve the equations modeling the fluid flow through the Discrete Fourier Transform (DFT). This approach can decouple the pressure from the Eq. 2, thus simplifying the computational solution, however, the numerical boundary condition have to be periodic since its use of FFT.

Applying the Fourier Transform on the continuity equation, Eq. 1, it is found the Eq. 4,

$$ik_j \hat{u}_j = 0 \tag{4}$$

where $i = \sqrt{-1}$, k_j is the wave number and $\hat{u}_j$ is the transformed velocity field j to the spectral space.

The Equation 4 shows that the product between two vectors is null, therefore the wave number k_j is orthogonal to the transformed velocity $\hat{u}_j$. Consequently, it is defined a π plane which is perpendicular with k_j and contains $\hat{u}_j$, Fig. 1.

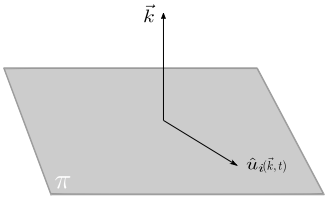

Figure 1. π plane

Applying DFT on the momentum linear equation, Eq. 2, and the properties of the Fourier transform, it is found Eq. 5,

$$\frac{\partial \hat{u}_i}{\partial t} + \frac{1}{2}\left(ik_j \widehat{u_i u_j} + \hat{u}_j \frac{\partial \hat{u}_i}{\partial x_j}\right) = -ik_i \hat{p} - \nu k^2 \hat{u}_i + \hat{f}_i, \tag{5}$$

where k^2 is the square norm of the wave number, *i.e.*, $k^2 = k_i k_j$.

The rate of change of linear momentum, $\frac{\partial \hat{u}_i}{\partial t}$, belong to the π plane as the viscosity term, $\nu k^2 \hat{u}_i$ in the reason of the π plane definition as the gradient pressure term, $ik_i\hat{p}$ is collinear with vector $\vec{k}$ and also perpendicular to the π plane. The position of the advective term, $\frac{1}{2}\left(ik_j\widehat{u_i u_j} + \hat{u}_j\frac{\partial \hat{u}_i}{\partial x_j}\right)$, in concern of the π plane is unknown as it is the position of the $\hat{f}_i$ in relation to the same plane.

In relation of the terms positions to the π plane, the Eq. 5 is rewrite into the Eq. 6,

$$\underbrace{\left(\frac{\partial}{\partial t} + \nu k^2\right)\hat{u}_i}_{\in\pi} + \underbrace{\frac{1}{2}\left(ik_j\widehat{u_i u_j} + \hat{u}_j\frac{\partial \hat{u}_i}{\partial x_j}\right) + ik_i\hat{p} - \hat{f}_i}_{\in\pi} = 0, \tag{6}$$

which indicates that the vector sum of advective, gradient pressure and source terms is collinear to the vector sum of the transient and difusive terms since the Eq. 6 is equals to zero, therefore, the two sums are in π plane.

Even though the vector sum of advective, gradient pressure and source terms is in π plane, it is required that vectors are also over the π plane and for that it is used the projection tensor concept. Applying this concept into the second sum highlighted in the Eq. 6, it is found Eq. 7,

$$\frac{1}{2}\left(ik_j\widehat{u_i u_j} + \hat{u}_j\frac{\partial \hat{u}_i}{\partial x_j}\right) + ik_i\hat{p} - \hat{f}_i = \varphi_{im}\left[\frac{1}{2}\left(ik_j\widehat{u_m u_j} + u_j\widehat{\frac{\partial u_m}{\partial x_j}}\right) + \hat{f}_m\right], \tag{7}$$

where $\varphi_{im} = \delta_{im} - \frac{k_i k_m}{k^2}$; $\delta_{im} = 1$ if $i = m$ and $\delta_{im} = 0$ if $i \neq m$.

The gradient pressure is perpendicular to the π plane, therefore the projection of this vector into the plane is null. After the Eq. 7 is included in the Eq. 6, it is found the Eq. 8,

$$\frac{\partial \hat{u}_i}{\partial t} = -\nu k^2\hat{u}_i + \varphi_{im}\left[-\frac{1}{2}\left(ik_j\widehat{u_m u_j} + u_j\widehat{\frac{\partial u_m}{\partial x_j}}\right) + \hat{f}_m\right]. \tag{8}$$

2.3 Numerical-Computational Methodology: Fourier Pseudo-Spectral Method (PFM)

The PFM consists in solving the non-linear term and the force term, $\hat{f}_m$ in the physical domain avoiding a convolution in the spectral domain while solving the diffusion term in the Fourier domain. Thus, this methodology provides high accuracy since the differential terms are solved as products in the spectral domain however there is no convolution causing high computational cost.

It is necessary a time advancement method of high order to level an approach such as PFM implemented in the IMERSPEC's spatial discretization. The method used in the present algorithm is the fourth-order 6 stages Runge-Kutta scheme (RK46). This scheme is shown in the Eq. 9,

$$\begin{cases} AUX_i^l = \alpha^l AUX_i^{l-1} + \Delta t\, RHS^l \\ \hat{u}_i^{l+1} = \hat{u}_i^l + \beta^l AUX_i^l \end{cases} \tag{9}$$

where *AUX* is an auxiliary variable, $l = 1, 2, \cdots, 6$ is the Runge-Kutta stage, *RHS* is the right hand side of the Eq. 8, α and β are shown in Tab. 1.

Table 1. RK46 Coefficients.

l	α	β
1	0,0	0,122
2	-0,691750960670	0,477263056358
3	-1,727127405211	0,381941220320
4	-0,694890150986	0,447757195744
5	-1,039942756197	0,498614246822
6	-1,531977447611	0,186648570846

The time increment, Δt, is defined in each temporal advancement based in the *Courant-Friedrich-Lewis* criterion (CFL). The expression of Δt is presented in Eq. 10,

$$\Delta t = CFL \cdot min \left\{ min \left[\frac{\Delta x}{max||u||}; \frac{\Delta y}{max||v||} \right]; \frac{2}{\nu} \left(\frac{1}{\Delta x^2} + \frac{1}{\Delta y^2} \right)^{-1} \right\}, \tag{10}$$

where $\Delta x = L_x/N_x$, $\Delta y = L_y/N_y$, L_x is the domain length in the x direction, L_y is the same measure in the y direction, N_x and N_y are the number of collocation points in correspond direction.

2.4 Immersed Boundary Method

This method is used to impose geometries or other boundary conditions in the flow domain besides the periodic ones. To employ the Immersed Boundary Method (IBM) is required two domains: an eulerian domain (Ω) where the flow is modeled and a lagrangian domain (Γ) where the predetermined geometry or boundary conditions are modeled.

The source term f_i is responsible for the communication between Γ and Ω. This variable, in Ω, is obtained isolating f_i in the Eq. 2, thus, it is obtained Eq. 11,

$$f_i = \frac{\partial u_i}{\partial t} + \frac{1}{2} \left[\frac{\partial (u_i u_j)}{\partial x_j} + u_j \frac{\partial u_i}{\partial x_j} \right] + \frac{\partial p}{\partial x_i} - \nu \frac{\partial^2 u_i}{\partial x_i \partial x_j}. \tag{11}$$

The continuity equation, Eq. 1 and the linear momentum equations, Eq. 2, are developed under the assumption of continuum hypothesis, hence in Γ there is also an identical equation to Eq. 11 with lagrangian variables (represented by capital letters in the present paper). This identical equation is presented by Eq, 12,

$$F_i = \frac{\partial U_i}{\partial t} + \frac{1}{2} \left[\frac{\partial (U_i U_j)}{\partial X_j} + U_j \frac{\partial U_i}{\partial X_j} \right] + \frac{\partial P}{\partial X_i} - \nu \frac{\partial^2 U_i}{\partial X_i \partial X_j}. \tag{12}$$

Considering an explicit Euler scheme as the advancement temporal method to IBM's comprehension purposes and grouping the Other Terms of the Equation in a variable, *OTE*. The Equation 12 may be rewrite as Eq. 13,

$$F_i(\vec{X}, t) = \frac{U_i^{t+\Delta t} - U_i^t}{\Delta t} + OTE_i^t. \tag{13}$$

The lagrangian force is determined by the Direct Forcing Method, this approach determine $F_i(\vec{X}, t)$ with the insertion of an estimated parameter, U_i^*, in the Eq. 13, *i.e.*,

$$F_i(\vec{X}, t) = \frac{U_i^{t+\Delta t} + U_i^* - U_i^* - U_i^t}{\Delta t} + OTE_i^t. \tag{14}$$

The Eq. 14 may be decomposed in two other equations,

$$\frac{U_i^* - U_i^t}{\Delta t} + OTE_i^t = 0, \tag{15}$$

$$F_i(\vec{X}, t) = \frac{U_i^{t+\Delta t} - U_i^*}{\Delta t}. \tag{16}$$

The term $U_i^{t+\Delta t}$ is the desirable velocity imposed to the flow, thus, this term is an open variable since it value depends of the implemented condition and it will be represent as U_{IB}.

Under continuum hypothesis assumption, the Eq. 15 has an identical expression in the Ω, presented by Eq. 17,

$$\frac{u_i^* - u_i^t}{\Delta t} + ote_i^t = 0. \tag{17}$$

This estimated eulerian velocity (u_i^*) is equal to the lagrangian one (U_i^*) if $\vec{x} = \vec{X}$ and $U_i^* = 0$ in case of $\vec{x} \neq \vec{X}$. After U_i^* determination and with the imposed U_{IB}, the lagrangian force, F_I, is calculated through Eq. 16.

The eulerian f_i is determined by the Eq. 3 and is applied in the Eq. 18,

$$u_i^{t+\Delta t} = u_i^t + f_i \Delta t. \tag{18}$$

This equation materializes from the Eq. 16 under continuum hypothesis to also be applied in Ω. The fluid velocity in the immersed boundary should be equal to U_{IB} however they are not since the temporal/spatial discretizations processes, interpolation/distribution process and mass conservation. For better accuracy, the direct forcing method is substituted by the multi-direct forcing method which repeat the direct forcing method until the fluid velocity in the eulerian domain tents to value of U_{IB}. Mariano (2011) and Moreira (2007) presents the IMERSPEC methodology with more details and also may be consulted.

3. RESULTS AND DISCUSSION

3.1 Verification

In the present paper it is simulated the Taylor-Green Vortex as a verification to the IMERSPEC. The Taylor-Green vortex were proposed since it is a manufactured solution, the flow continuum solution is presented through Eq. 19, 20 and 21,

$$u_{TG} = U_\infty \sin\left(\frac{ax}{L}\right) \cos\left(\frac{by}{L}\right) e^{-\left[\frac{\nu t}{L^2}(a^2+b^2)\right]}, \tag{19}$$

$$v_{TG} = -U_\infty \frac{a}{b} \cos\left(\frac{ax}{L}\right) \sin\left(\frac{by}{L}\right) e^{-\left[\frac{\nu t}{L^2}(a^2+b^2)\right]}, \tag{20}$$

$$p_{TG} = -\rho U_\infty^2 \frac{a^2}{2b^2} \left[\sin^2\left(\frac{ax}{L}\right) - \cos^2\left(\frac{by}{L}\right)\right] e^{-\left[\frac{2\nu t}{L^2}(a^2+b^2)\right]}, \tag{21}$$

where the vortices size, L, are $\pi\, m$, the domain size is $2Lx2L$, the velocity U_∞ is $1\, m/s$ and the Reynolds number, *Re*, is 10. The simulations were performed for $3\pi\, s$ physical, $CFL = 0.75$ and a mesh with $16x16$ collocation points. The initial conditions for u_{TG}, v_{TG} and p_{TG} are shown in the Fig. 2, 3 and 4.

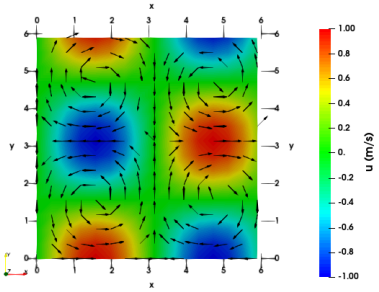

Figure 2. Initial condition of u_{TG}

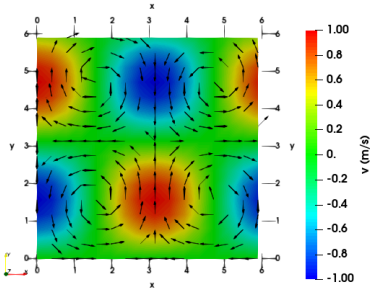

Figure 3. Initial condition of v_{TG}

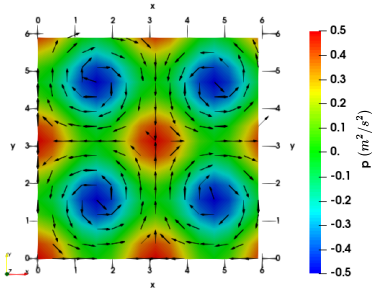

Figure 4. Initial condition of p_{TG}

There were performed two types of virtual experiments considering the Green-Taylor Vortices, one without IBM and the other with IBM. To evaluate the IMERSPEC accuracy is used the norm L_2, Eq. 22,

$$L_2 = \sqrt{\frac{\sum_{i=1}^{N_x}\sum_{j=1}^{N_y}(\phi_{ij}^c - \phi_{ij}^n)}{N_x N_y}}, \tag{22}$$

where the superscript *c* corresponds to the continuum variable and *n* to the computational-numerical one.

The Figure 5, 6 and 7 shows the pressure and velocity u and v in $t = \pi/4\, s$ without IBM. Comparing this figures with the initial condition is shown that the vortices are spreading over physical time.

The L_2 norm for u, v and p is presented in the Fig. 8 over t/t_f and $t_f = 3\pi\, s$. Through Fig. 8 is shown that the norm for u and v are in agreement and all the norms presents machine error accuracy indicating high accuracy in the IMERSPEC2D methodology.

The second virtual experiment performed had a lagrangian domain inside an eulerian domain, Fig. 10. The immersed boundary applied the continuum values of u_{TG} and v_{TG} into the eulerian coincided points during the simulation.

This virtual experiment showed the same modeled behavior observed in Fig. 5, 6 and 7 however the L_2 norm over t/t_f shows that the lagrangian points increased the method's accuracy.

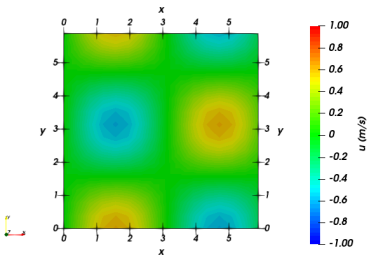

Figure 5. u in $t = \pi/4\,s$

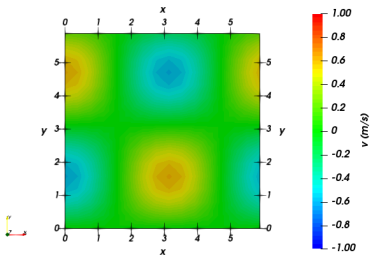

Figure 6. v in $t = \pi/4\,s$

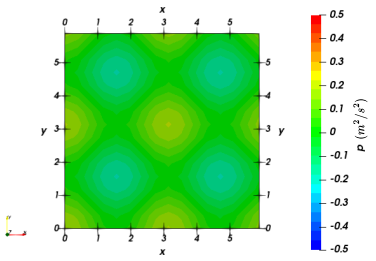

Figure 7. p in $t = \pi/4\,s$

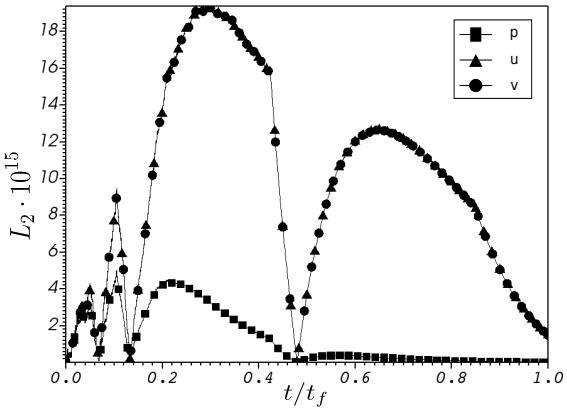

Figure 8. L_2 for u, v and p for simulation without IBM

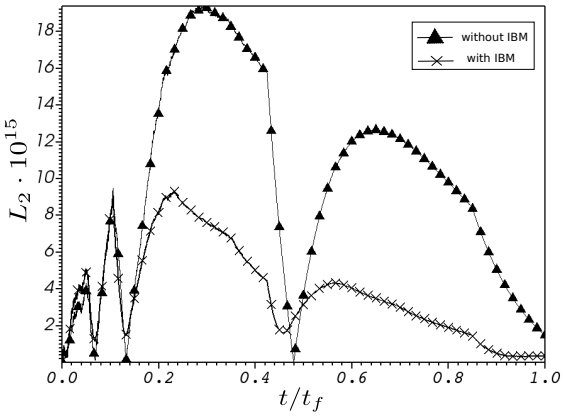

Figure 9. Comparing component u L_2

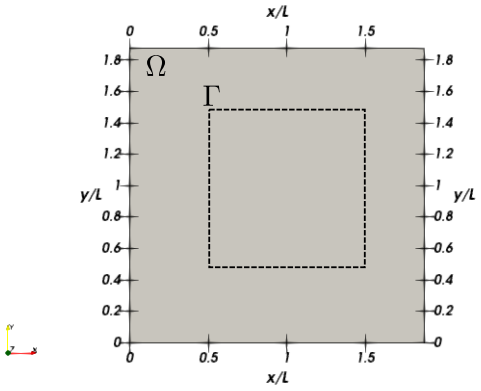

Figure 10. Eulerian and lagrangian domain for Taylor-Green Vortices

3.2 Temporal Plane Jet

The temporal jets are simulated to show the IMERSPEC approach in a canonical flow virtual experimentation. The jet implemented was a plane one, this type of flow originates from the discharged of fluid from a two-dimensional nozzle of width D and height H. The nozzle height H is larger than the with D and thus the flow is presumed essentially two-dimensional during part of its developed (Thomas, 1991).

The temporal aspect of the flow is presumed as a lagrangian approach which the model follows the fluid particle along its spread.

The initial condition implemented to the temporal jet is zero for velocity v component and pressure while for the velocity u component was implemented the Eq. 23,

$$u_0(x,y) = \frac{u_\infty + u_{cf}}{2} - \frac{u_\infty - u_{cf}}{2} \tanh\left[\frac{R}{4\theta}\left(\frac{|y|}{R} - \frac{R}{|y|}\right)\right], \tag{23}$$

where u_∞ is the inlet velocity of the jet, u_{cf} is the co-flow velocity, R is the jet radius and θ is the shear momentum thickness. The values of the variables used in the present paper are shown in the table 2.

Table 2. Jet properties.

u_∞	u_{cf}	R	θ
$1\,m/s$	$0\,m/s$	$0.5\,m$	0.025

The rate R/θ defines the profile velocity's inclination which has strong impact in the transition process to turbulence, overall a hight rate indicates more instabilities on the jet (Moreira, 2007). In the present paper, it was adopted a rate $R/\theta = 20$.

The temporal jet was simulated with 10, 100 and 1600 Reynolds numbers, Re,

$$Re = \frac{(u_\infty - u_{cf})\delta_0}{\nu}, \tag{24}$$

$\delta_0 = 1.187\,m$ and is the initial shear layer thickness and ν is the kinematic viscosity. The virtual experiments modeled the flow during $60\,s$ physical. The Figure 11 shows the initial condition implemented for the temporal jet on a $20Dx10D$ domain and the profile applied over all domain, Fig. 12.

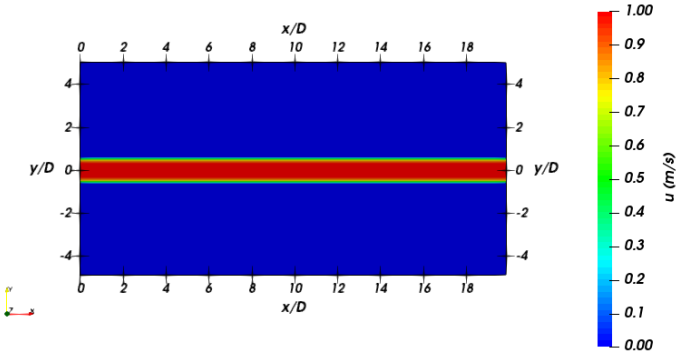

Figure 11. Jet's initial condition, $Re = 10$ and 128x64 points.

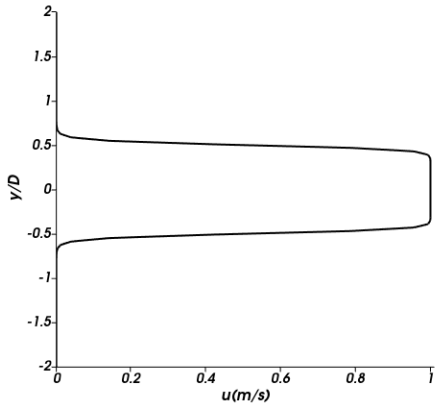

Figure 12. Jet's initial profile without noise.

Random noise is implemented over δ_0 to perturb the flow as its shown in Eq. 25,

$$\begin{cases} u(x,y) = u_0(x,y) + 5\left(\frac{0.5-a}{100}\right), \\ v(x,y) = 5\left(\frac{0.5-a}{100}\right), \end{cases} \tag{25}$$

where a is a random number between 0 and 1 (Moreira, 2007).

For $Re = 1600$, it was performed simulations with $128x64$, $256x128$ and $512x256$ collocation points and noise in the initial shear layer thickness, as shown in Eq. 25. The results obtained in $t = 16\,s$ are shown in Fig. 13, 14 and 15. It is clear that all meshes were able to express the Kelvin-Helmholtz instabilities yet the structures' sharpness were increased with the mesh refinement. Since all meshes are able to model the characteristic instabilities of this flow's type, the subsequent analysis are performed with $256x128$ collocation points since this mesh presents the same sharpness from the most refine one and offers better results than the least refine mesh.

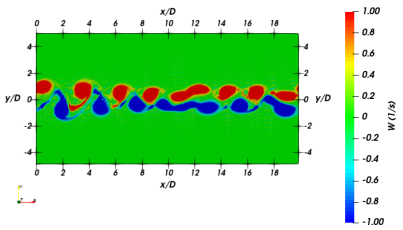

Figure 13. $\vec{W}$ for $128x64$ points.

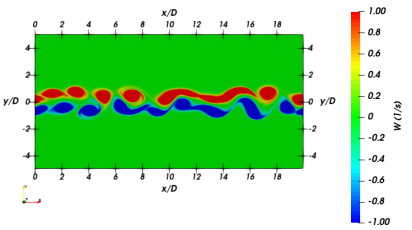

Figure 14. $\vec{W}$ for $256x128$ points.

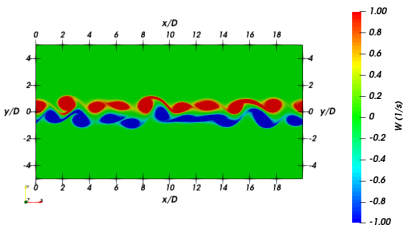

Figure 15. $\vec{W}$ for $512x256$ points.

Figures 16, 17, 18 and 19 presents the results obtained by Souza *et al.* (2005) for a temporal jet with $Re = 1600$ in $3D$ code and a mesh with 120^3 collocation points.

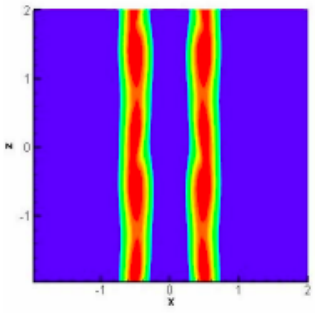

Figure 16. $||\vec{W}||$ in 5 s.

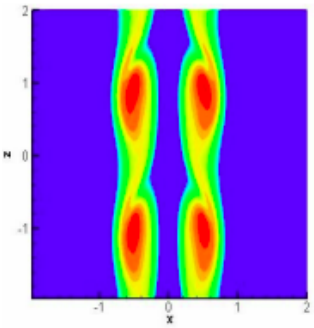

Figure 17. $||\vec{W}||$ in 10 s.

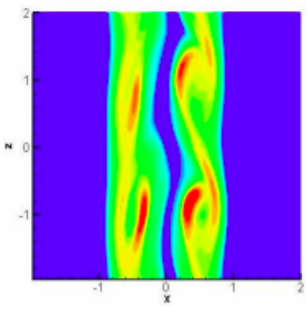

Figure 18. $||\vec{W}||$ in 20 s.

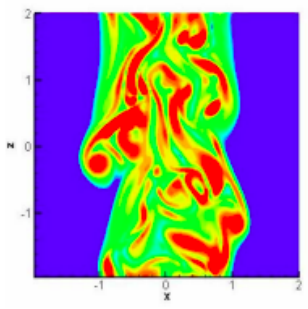

Figure 19. $||\vec{W}||$ in 30 s.

Figures 20, 21, 22 and 23 shows the temporal jet with $Re = 1600$ simulated in the present paper in the same physical time of the figures 16-19.

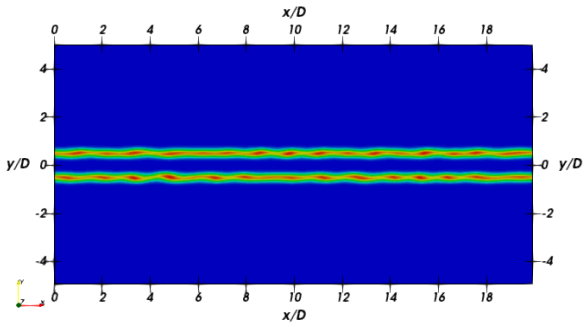

Figure 20. $||\vec{W}||$ in 5 s.

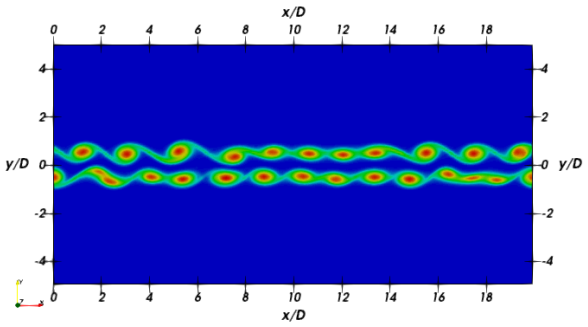

Figure 21. $||\vec{W}||$ in 10 s.

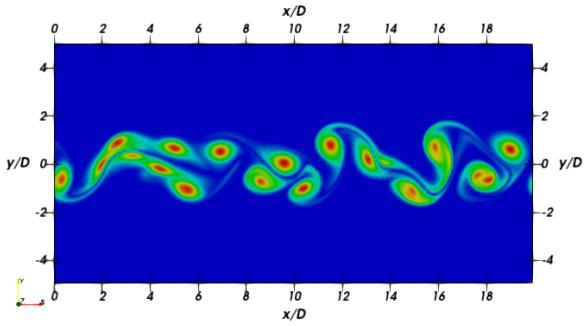

Figure 22. $||\vec{W}||$ in 20 s.

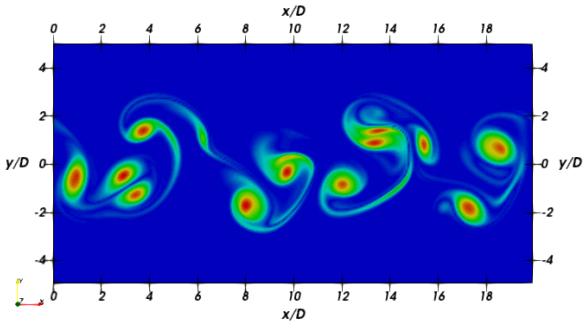

Figure 23. $||\vec{W}||$ in 30 s.

The jet's flow with Reynolds number equals to 1600 is considered turbulent however the flow start laminar at the nozzle's outlet. Physical intrinsic perturbations are introduced in the inflectional field of $\vec{V}$ and thus a process is developed which selects a wave-length and its will be more amplified by the flow resulting in a first Kelvin-Helmholtz instability. This instability causes the shear layer winding. It is relevant to highlight that all the spectrum which corresponds to the flow's perturbations are amplified yet with different amplified rates (Silveira Neto, 2020).

During the amplification process, two instabilities may pair causing a new winding which form new bigger structure. This new bigger structure also presents Kelvin-Helmholtz instabilities inside itself, this is denominated by an eddy. After this new formation, the flow develops, under unknown reasons, longitudinal filaments, and these filaments curl up around the eddies during its stretch. After this process, the flow's instabilities keep amplifying until reach a turbulent stage however the jet's flow became three-dimensional.

The commented process is illustrated in part by the Fig. 16-19. Comparing the results obtained in the present paper and those presented by Souza *et al.* (2005), it is reasonable to conclude that the IMERSPEC2D may model the physical flow until its instabilities became three-dimensional, thus, Fig. 22 and 23 have not physical meaning.

The random noise implemented in δ_0 has an important aspect in the physical modeling, as already said, the transition to turbulence begins with flow perturbations. The IMERSPEC2D presents error machine accuracy as showed in Fig. 9

thus there are not any perturbations to be amplified as there is in other spatial methodologies such as finite volume method.

Figures 24-26 presents the $||\vec{W}||$ in $t = 60\,s$ for the IMERSPEC2D's results operating without noise. The figures shows that the flows did not develop any instabilities over the simulated time. Figures 27-29 indicates the results obtained from IMERSPEC2D under random noise implementation, Eq. 25.

For jets under laminar regime, even when random noise is implemented the flows' behavior does not suffer any change as may be seen comparing Fig. 24 and 27.

Perturbations are significant in the jet flow for $Re = 100$, as it is observed comparing Fig. 25 e 28, yet there are not any formation of Kelvin-Helmholtz instabilities. The flow appear to be in an unstable laminar regime.

Finally, for the flow with $Re = 1600$ the Kelvin-Helmholtz developed only under random noise, Fig. 29, however, the transition to the turbulent regime does not advance since the code is two-dimensional and is not able to model three-dimensional instabilities.

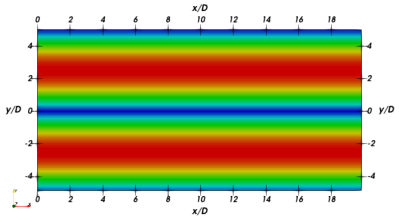

Figure 24. $Re = 10$ without noise.

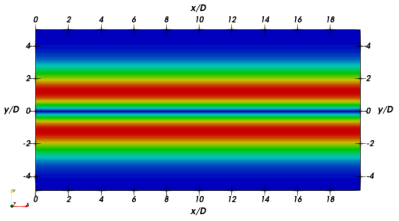

Figure 25. $Re = 100$ without noise.

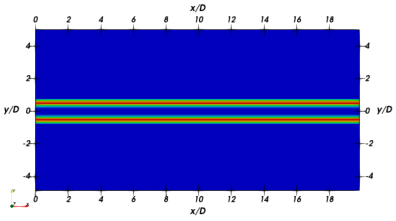

Figure 26. $Re = 1600$ without noise.

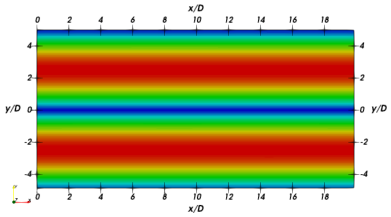

Figure 27. $Re = 10$ with noise.

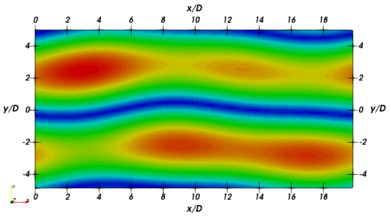

Figure 28. $Re = 100$ with noise.

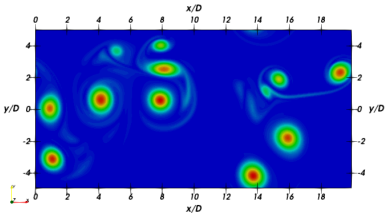

Figure 29. $Re = 1600$ with noise.

4. CONCLUSION

The present paper sought to validate the IMERSPEC2D code through the verification process with Taylor-Green vortices, a manufactured solution, and temporal plane jet simulations.

The verification indicated the IMERSPEC method's high accuracy with or without the use of IBM since both the L_2 norm u velocity component presented machine error magnitude.

The pressure decoupling in the IMERSPEC approach besides its high accuracy is a significant characteristic. In the simulations performed, the pressure became a variable calculated in the post processing.

For the temporal plane jet, it was concluded that the IMERSPEC is able to model unperturbed laminar plane jet flow, however for perturbed laminar, in transition or turbulent plane jets the methodology needs imposed perturbations. This perturbations was modeled by a random noise applied in the initial shear layer thickness for u and v.

Finally, the IMERSPEC2D code can model temporal turbulent plane jets only before its instabilities becomes three-dimensional. When the flow becomes three-dimensional the results obtained by the code has no physical meaning.

5. ACKNOWLEDGEMENTS

The authors thank the Coordenação de Aperfeiçoamento de Pessoal de Nível Superior – Brasil (CAPES), the Faculdade de Engenharia Mecânica (FEMEC) of Universidade Federal de Uberlândia (UFU), the Escola de Engenharia: Elétrica, Mecânica e de Computação (EMC) of the Universidade Federal de Goiás (UFG) for they support, FURNAS Centrais Elétricas and the "Programa de Pesquisa e Desenvolvimento Tecnológico" (P&D) of the ANEEL for the financial support.

6. REFERENCES

Mariano, F.P., 2011. *Numerical Solution of Navier-Stokes Equations using a Hybrid Methodology of Immersed Boundary and Fourier Pseuso-Spectral*. Ph.D. thesis, Universidade federal de Uberlândia, Uberlândia, Minas Gerais, Brasil.

Moreira, L.d.Q., 2007. *Large Eddy Simulation of Periodic Temporal Jets Using the Fourier Pseudo-Spectral Method*. Master's thesis, Universidade Federal de Uberlândia, Uberlândia, Minas Gerais, Brasil.

Silveira Neto, A., 2020. *Escoamentos Turbulentos: Análise Física e Modelagem Teórica*. Composer, Uberlândia, Minas Gerais, Brasil, 1st edition.

Souza, A.M.d. *et al.*, 2005. *Análise numérica da transição à turbulência em escoamentos de jatos circulares livres*. Ph.D. thesis, Universidade federal de Uberlândia, Uberlândia, Minas Gerais, Brasil.

Thomas, F.O., 1991. "Structure of mixing layers and jets". *Applied Mechanics Reviews*.

7. RESPONSIBILITY NOTICE

The authors are solely responsible for the printed material included in this paper.